

Tunable two-photon pumped lasing using a holographic polymer-dispersed liquid-crystal grating as a distributed feedback element

Guang S. He,^{a)} Tzu-Chau Lin, Vincent K. S. Hsiao, Alexander N. Cartwright, and Paras N. Prasad

Institute for Lasers, Photonics and Biophotonics, The State University of New York at Buffalo, Buffalo, New York 14260-3000

L. V. Natarajan,^{b)} V. P. Tondiglia,^{b)} R. Jakubiak, R. A. Vaia, and T. J. Bunning

Air Force Research Laboratory, Materials and Manufacturing Directorate, Wright-Patterson Air Force Base, Ohio 45433-7500

(Received 15 May 2003; accepted 6 August 2003)

A holographic polymer-dispersed liquid-crystal (H-PDLC) grating film was employed as an angle-dependent and narrow spectral-band feedback control element for two-photon pumped lasing in a dye solution, 4-[N-(2-hydroxyethyl)-N-(methyl)amino phenyl]-4'-(6-hydroxyhexyl sulfonyl) stilbene (APSS) in dimethyl sulphoxide. The grating film contained about 80 layers of liquid-crystal domains periodically dispersed in an $\sim 15 \mu\text{m}$ thick polymer film, featuring a maximum reflectance of 75% at 561 nm position with an $\sim 9 \text{ nm}$ spectral bandwidth. The output lasing wavelength could be tuned from 561.5 to 548.5 nm and the lasing bandwidth changed from 5 to 3 nm when the incidence angle on the grating film varied from 0° to 22° . The overall lasing efficiency was measured to be 10%. © 2003 American Institute of Physics. [DOI: 10.1063/1.1615315]

The tendency toward miniaturization in the emerging generation of nanoscale opto-electronic devices creates a demand for morphologically precise photonic structures, for example, photonic band-gap materials and microcavities. Holographic photopolymerization has proven to provide rapid multidimensional morphology control of organic and organic/inorganic hybrid systems on length scales commensurate with the writing wavelengths, thus potentially impacting a wide range of visible and near-infrared photonic applications. Holographic polymer-dispersed liquid-crystal (H-PDLC) systems are a recent technological example of the versatility of holographic photopolymerization for photonics.^{1,2} Interference from two laser beams creates a standing intensity pattern within a photoreactive formulation. In regions of constructive interference, the rate of photopolymerization is greatest, leading to preferential phase segregation of the liquid-crystal (LC) component in the form of nanosized droplets in the regions of destructive interference, thus creating a morphological replica of the original intensity pattern comprised of LC droplet-rich and cross-linked polymer-rich lamellae. Moreover, the use of greater than two beams allows for the facile formation of two-dimensional and three-dimensional photonic crystals where the crystal symmetry is dictated by the writing amplitudes, geometry, and writing beam polarizations.^{3,4} Spectral agility of the peak transmission or reflection wavelength of this kind of device can be realized by applying an electric field or changing the incidence angle of the light beam.⁵

Technologically separated from H-PDLCs, a number of dye compounds have been developed in the recent decade, which can be used as highly efficient two-photon-pumped

(TPP) lasing materials.^{6–11} So far, most reports of TPP lasing were based on a fixed lasing wavelength for a given dye-activated gain medium, which usually provided a spectral linewidth of 14–20 nm for cavityless lasing or 10–15 nm for cavity lasing without using a grating as dispersion element.

In this letter, we report the tunable TPP cavity lasing performance using a high-quality H-PDLC grating film as an angle-dependent and spectrally selective distributed feedback element that could significantly reduce the cavity lasing spectral linewidth.

The experimental setup of our tunable cavity lasing system is schematically shown in Fig. 1. The gain medium employed in this study was a dye solution 4-[N-(2-hydroxyethyl)-N-(methyl)amino phenyl]-4'-(6-hydroxyhexyl sulfonyl) stilbene (APSS) in dimethyl sulphoxide.⁶ The pump source was a pulsed dye laser system providing lasing output of $\sim 815 \text{ nm}$ wavelength, $\sim 8 \text{ ns}$ pulse duration, $\sim 1 \text{ mrad}$ beam divergence, $\sim 2 \text{ mm}$ beam size, and 10 Hz repetition rate. The IR pump beam was focused via a $f=20 \text{ cm}$ lens onto the center of a 2 cm long glass cell filled with

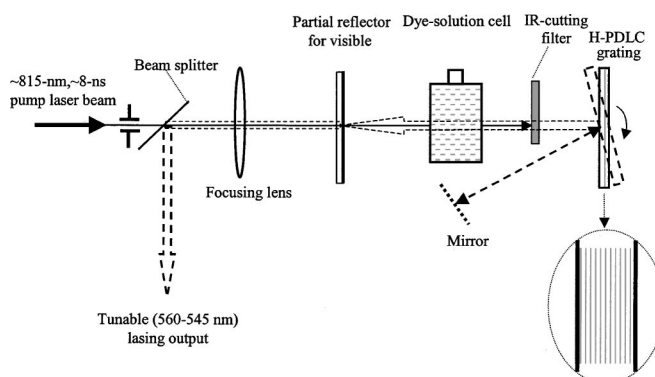


FIG. 1. Experimental setup for two-photon pumped cavity lasing using a H-PDLC grating film as an angle-tunable feedback element.

^{a)}Electronic mail: gshe@acsu.buffalo.edu

^{b)}Also at: Science Applications International Corporation, Dayton, OH 45431.

APSS dye solution of 0.06 M/L concentration. The cavity for TPP lasing was basically formed by a front partial reflection mirror, which was highly transparent ($T \approx 95\%$) for the 815 nm pump beam and partially reflective ($R \approx 60\%$) for the 560–540 nm beam, and a H-PDLC grating film as an angle-tunable back reflector with an extremely narrow spectral band. The backward TPP lasing was coupled out via a beam splitter.

The H-PDLC grating employed in this study was formed through anisotropic phase separation of nanoscale liquid-crystal domains from the polymer matrix by using holographic photopolymerization techniques employing thiol-ene chemistry. The prepolymer formulation consisted of a commercially available thiol-ene formulation (NOA 65 from Norland, Cranbury, NJ), 30%–32% of a nematic liquid-crystal BL037 (EM Industries, Hawthorne, NY) with 1% Irgacure 4265 UV initiator. Although the commercial NOA 65 has a proprietary UV initiator, only weak reflection gratings with diffraction efficiencies (DE) $< 20\%$ were obtainable. The addition of Irgacure 4265 UV initiator greatly enhances the DE ($> 70\%$) for the same UV power. Thin sample cells were made from Corning 1737 glass plates using 15 μm glass spacers. Writing of the grating was done using a Coherent Ar-ion laser Model 308C at a laser wavelength of 363.8 nm with an output power of ~ 200 mW. The UV laser beam was expanded to a 5 mm diameter using a $4\times$ microscope objective. The gratings were written by a single-laser beam in conjunction with an isosceles 90° glass prism. As a result of the interference between the incident beam and its own total internal reflection, an intensity pattern with periodic variation of high and low intensities was created on the sample cell. Photopolymerization leads to the phase separation of the liquid crystal into droplets and there is separation of LC-rich and polymer-rich regions. Reflection gratings are formed due to the index modulation created by alternating layers of LC and polymer.^{1,12} The cell was placed in optical contact with the prism hypotenuse using an index matching fluid. The exposure time was typically 30 s. The entrance face of the prism was at 45° to the cell. In its final form for the cavity lasing application, the H-PDLC grating film was covered by two glass plates with the grating planes parallel to the film surface. The grating film was approximately 15 μm thick and contained approximately 80 periods of the phase separated polymer/LC planes.

Shown in Fig. 2 is a bright-field transmission electron micrograph of an ultramicrotomed section of a reflective H-PDLC film showing the internal morphology consisting of planes of cross-linked polymer (light areas) separated by LC-droplet-rich regions (dark areas). Individual PDLC domains with diameters between 50–75 nm are confined to regions approximately 90 nm in width separated by approximately 90 nm of cross-linked polymer. The fraction of the period composed of the active component is approximately 50% and little polymer within the active region is observed. The grating period of ~ 180 nm is expected for a Bragg wavelength of 560 nm.

Figure 3 shows the measured transmission curves of the grating film at three different incidence angles (between the input light beam and the normal of film surface); these curves were obtained by using a scanning spectrometer with

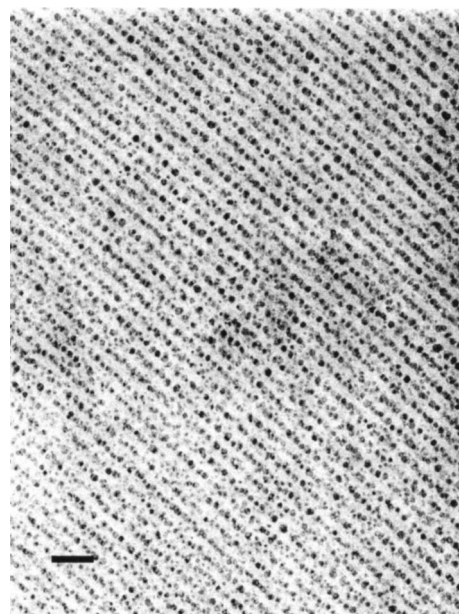


FIG. 2. Bright-field transmission electron micrograph of a thin section from a reflective H-PDLC film. Scale bar=500 nm.

~ 1 nm resolution. From Fig. 3, one can see that at normal incidence ($\theta=0^\circ$) the maximum reflection from the grating film was $\sim 75\%$ at the wavelength position of 560.5 ± 0.5 nm. The maximum reflection wavelength position shifted to the short-wavelength side when the incident angle was increased. For example, at $\theta=10^\circ$, 20° , and 30° , the measured maximum reflection wavelengths were 558, 549.5, and 535 ± 0.5 nm, respectively. The spectral full width at half maximum (FWHM) of the maximum reflectance band for a given incidence angle was ~ 9 nm. It should be noted in Fig. 3 that the background curve shape outside the narrow maximum reflectance band was determined by the glass–air interface reflection and the additional scattering loss due to multiple liquid-crystal layers. It is known that the latter is highly dependent on the wavelength, i.e., the shorter is the incident wavelength, the greater is the scattering loss.

Figure 4 shows the measured spectra of [Fig. 4(a)] the side fluorescence emission, [Fig. 4(b)] the amplified spontaneous emission [(ASE) or single-pass stimulated emission

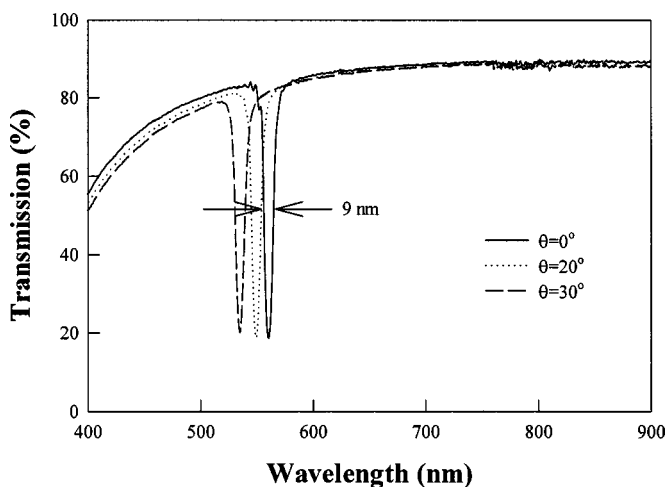


FIG. 3. Spectral transmission curves of the H-PDLC grating film at three different incident angles.

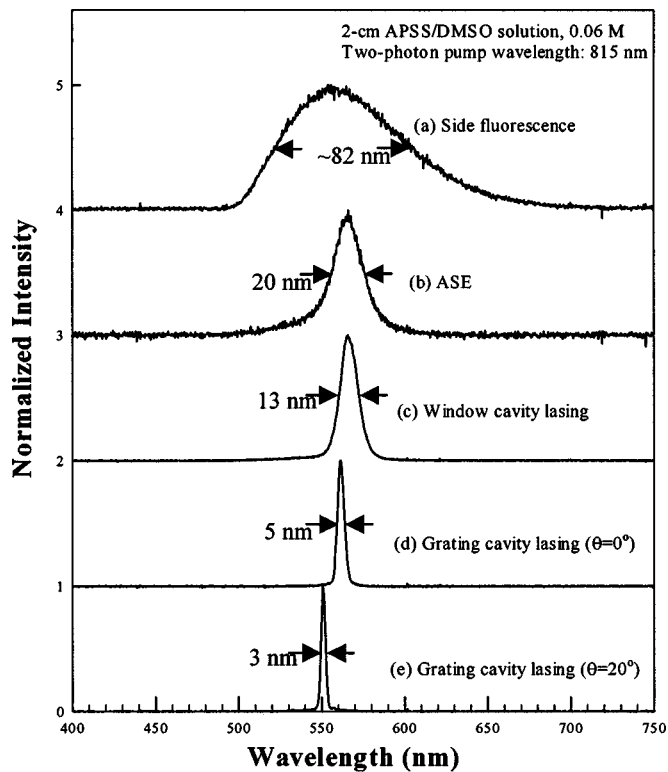


FIG. 4. Spectra of the side fluorescence (curve a), ASE or cavityless lasing (curve b), cavity lasing formed by two windows of the cell (curve c), and the grating cavity lasing at two different incident angles (curves d and e).

without any feedback from mirrors or windows], [Fig. 4(c)] the cavity lasing with feedback from two windows of the dye cell, and [Figs. 4(d) and 4(e)] lasing at two different incidence angles from the cavity containing the grating. In Fig. 4, one can readily find that the spectral width of the grating cavity lasing is significantly reduced to 5–3 nm compared to that of the ASE or regular cavity lasing (20–13 nm).

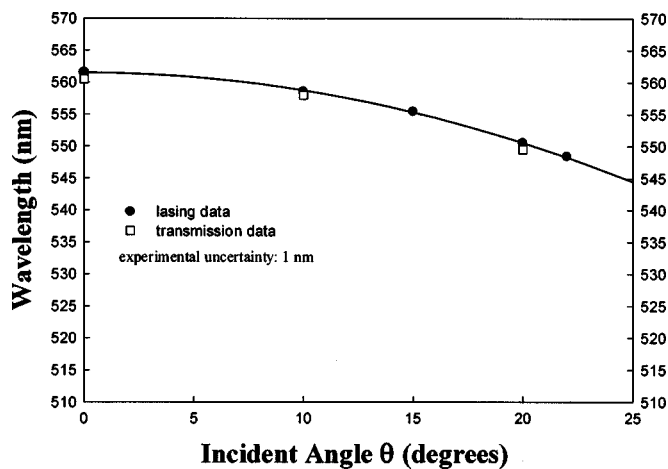


FIG. 5. Measured lasing tuning curve.

The measured lasing tunability curve is shown in Fig. 5, where the black dots represent the actual lasing wavelengths as a function of incidence angles while the hollow squares represent the maximum reflectance wavelengths at different incidence angles measured by a transmission spectrometer, as mentioned above. The two groups of data are nearly coincident within the experimental uncertainty of ± 0.5 nm. In our case, the maximum tunable angle was limited to $\theta=22\text{--}25^\circ$, beyond which the cavity lasing becomes more difficult probably due to the maximum reflectance wavelength being outside of the gain maximum position.

The near-field size (FWHM) of the output lasing beam was about 1.7 mm, and its far-field size was about 0.25 mm (after a $f=50$ cm focusing lens) that corresponded to a beam divergence angle of ~ 0.5 mrad. This measured divergence angle is nearly equal to the diffraction limit (~ 0.4 mrad) of an ~ 1.7 mm unfocused laser beam, suggesting a single-transverse-mode operation.

Finally, at 2 mJ input pump energy level, the output energy for the grating cavity lasing was measured to be $200 \mu\text{J}$, corresponding to an overall lasing efficiency $\eta=10\%$. At this pump level, the single-pass two-photon absorption ratio was 0.45. Therefore, the net conversion efficiency from the absorbed pump energy to the output lasing energy should be $\eta'=\eta/0.45\approx 22\%$.

In conclusion, we have demonstrated the high efficiency, wavelength selectivity, and tunability of two-photon pumped lasing by using a H-PDLC grating film that may additionally offer the advantage of electrical switchability.

This work was supported by the Air Force Office of Scientific Research and the Air Force Research Laboratory, Materials and Manufacturing Directorate. The technical assistance from Michael Pan and David Tomlin is acknowledged.

- ¹T. J. Bunning, L. V. Natarajan, R. L. Sutherland, and V. P. Tondiglia, *Annu. Rev. Mater. Sci.* **30**, 83 (2000).
- ²G. P. Crawford, *Opt. Photonics News* **14**, 54 (2003).
- ³R. L. Sutherland, V. P. Tondiglia, L. V. Natarajan, S. Chandra, and T. J. Bunning, *Opt. Express* **10**, 1074 (2002).
- ⁴M. J. Escuti, J. Qi, and G. P. Crawford, *Opt. Lett.* **28**, 522 (2003).
- ⁵R. Jakubiak, T. J. Bunning, R. A. Vaia, L. V. Natarajan, and V. P. Tondiglia, *Adv. Mater. (Weinheim, Ger.)* **15**, 241 (2003).
- ⁶G. S. He, J. D. Bhawalkar, C. F. Zhao, C.-K. Park, and P. N. Prasad, *Opt. Lett.* **20**, 2393 (1995).
- ⁷G. S. He, L. Yuan, Y. Cui, M. Li, and P. N. Prasad, *J. Appl. Phys.* **81**, 2529 (1996).
- ⁸G. S. He, K.-S. Kim, L. Yuan, N. Cheng, and P. N. Prasad, *Appl. Phys. Lett.* **71**, 1619 (1997).
- ⁹G. S. He, R. Signorini, and P. N. Prasad, *IEEE J. Quantum Electron.* **34**, 7 (1998).
- ¹⁰A. Abbotto, L. Beverina, R. Bozio, S. Bradamante, C. Ferrante, G. A. Pagani, and R. Signorini, *Adv. Mater. (Weinheim, Ger.)* **12**, 1963 (2000).
- ¹¹Y. Ren, Q. Fang, W.-T. Yu, H. Lei, Y.-P. Tian, M.-H. Jiang, Q.-C. Yang, and T. C. W. Mak, *J. Mater. Chem.* **10**, 2025 (2000).
- ¹²L. V. Natarajan, C. K. Shepherd, D. M. Brandelik, R. L. Sutherland, S. Chandra, V. P. Tondiglia, D. Tomlin, and T. J. Bunning, *Chem. Mater.* **15**, 2477 (2003).